Nonlinear Optical Polymers. 2. Novel NLO Linear Polyurethane with Dipole Moments Aligned Transverse to the Main Backbone

Naoto Tsutsumi,* Osamu Matsumoto, Wataru Sakai, and Tsuyoshi Kiyotsukuri

Department of Polymer Science & Engineering, Kyoto Institute of Technology, Matsugasaki, Sakyoku, Kyoto 606, Japan

Received July 25, 1995; Revised Manuscript Received October 19, 1995[⊗]

ABSTRACT: This paper presents a novel class of nonlinear optical (NLO) polymer for second harmonic generation (SHG). This new class of NLO polymer consists of the linear polyurethane, T-polymer, of tolylene 2,4-diisocyanate (TDI) with 3-[(2-hydroxyethyl)amino]-5-(hydroxymethyl)-4′-nitroazobenzene (T-AZODIOL), whose dipole moment is aligned transverse to the main chain backbone. For comparison, the linear polyurethane L-polymer, whose NLO chromophore is incorporated into the main chain, is synthesized from TDI with 4-[*N*-(2-hydroxyethyl)-*N*-methylamino]-3′-(hydroxymethyl)azobenzene (AZO-DIOL). T-polymer poled at optimum conditions of a corona poling voltage 8.0 kV, a temperature of 95 °C, and a time of 60 min shows a large second-order nonlinearity of $d_{33} = 1.6 \times 10^{-7}$ esu (67 pm/V) with good thermal stability at room temperature. The oriented NLO dipole moments for T-polymer do not show significant relaxation at ambient conditions after 60 days except for small depression a few days after poling, whereas, the SHG activity of L-polymer is largely decayed at room temperature. The better thermal stability of this new class of T-polymer is related to the smaller free volume in T-polymer.

Introduction

Organic nonlinear optical (NLO) materials have been extensively studied because of their potential application in integrated optical signal processing, and optical switching, etc. Poled polymeric materials are promising materials for second-order NLO materials. They have large susceptibilities, fast response times, excellent mechanical and physical properties, and good to be process ability. However, aligned NLO chromophores in polymeric materials are subject to thermal relaxation which leads to the reorientation of NLO chromophores in the matrix.

Several strategies have been presented for fabricating NLO polymer materials.[1−12] The first approach is the use of doping of an NLO chromophore into a polymeric matrix (guest−host system).[1−3] Second is the utilization of the polymer system with a pendant side group to which the NLO chromophore is covalently attached.[4] Third is the use of the polymer system with the NLO chromophore incorporated along the main chain backbone.[5] Furthermore, the cross-linking technique has been used to suppress the reorientation of an NLO chromophore due to molecular motion.[6−11] Recently, a new class of main chain polymer has been presented, where one head of the NLO unit is embedded in the polymer backbone and the dipole moments extend transverse to the main chain.[12]

We have synthesized a new type of NLO chromophore whose dipole moment is aligned transverse to the main chain backbone and found that the resultant poled polymer film has a large second harmonic efficiency with good thermal stability at the ambient conditions. The present NLO chromophore is based on an azobenzene dye. As pointed out by the previous work,[12] an NLO chromophore in this arrangement can be easier to orient by an external electric field than in structures where the dipole moments are pointing along the polymer backbone. Namely, the system whose NLO dipole moments aligned transverse to the polymer backbone requires less deformation of the main chain backbone on orienting the dipole moment to the poling field direction than does the system whose NLO dipole moment is incorporated along the polymer backbone. In this paper, we present the synthesis and the SHG

Scheme 1

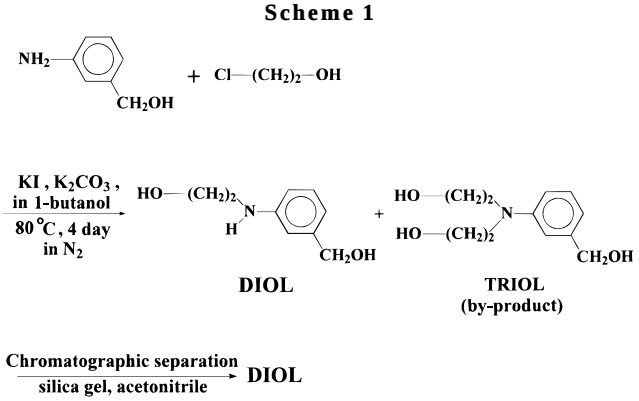

Scheme 2

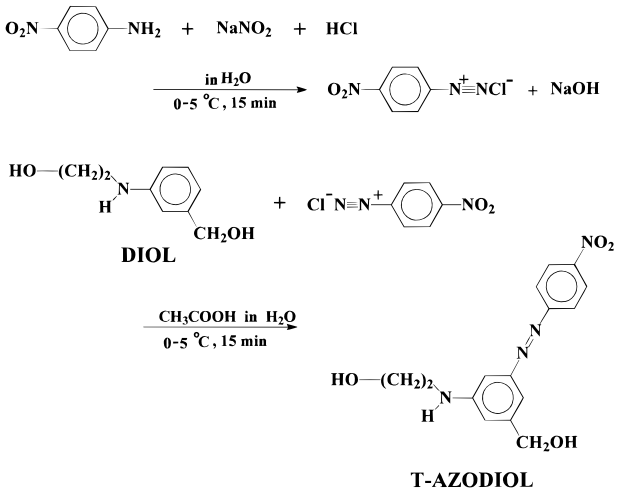

* To whom all correspondence should be addressed.

[⊗] Abstract published in *Advance ACS Abstracts,* December 1, 1995.

0024-9297/96/2229-0592$12.00/0

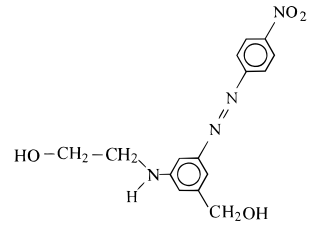

T-AZODIOL

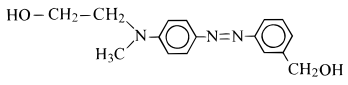

AZODIOL

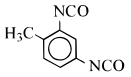

TDI

Figure 1. Chemical structures and codes of monomers for this study.

properties of this novel type of NLO polymer material whose dipole moments are transversely aligned to the main chain backbone and compare these properties with those for the polymer with an NLO chromophore in the main chain backbone.

Experimental Section

Materials. 3-[(2-Hydroxyethyl)amino]-5-(hydroxymethyl)-4′-nitroazobenzene (T-AZODIOL) was used as the NLO chromophore whose dipole moment is aligned transverse to the main chain backbone. T-AZODIOL was synthesized via two-step reactions shown in Schemes 1 and 2; First, 3-[(2-hydroxylethyl)amino]benzylalcohol (DIOL) was prepared from *m*-aminobenzyl alcohol with 2-chloroethanol. Then the coupling reaction of DIOL with diazotized *p*-nitroaniline gave rise to T-AZODIOL. The details of the synthesis procedure are shown below. 4-[*N*-(2-Hydroxyethyl)-*N*-methylamino]-3′-(hydroxymethyl)azobenzene (AZODIOL) dye was the NLO chromophore monomer for preparing the polymer with NLO chromophore incorporated in the main chain backbone. The detailed synthesis procedure of AZODIOL was given in our literature.[11] Commercially available tolylene 2,4-diisocyanate (TDI) was used without further purification. The chemical structures of the monomers are shown in Figure 1.

3-[(2-Hydroxyethyl)amino]benzyl Alcohol (DIOL). Scheme 1 shows the synthesis procedure of 3-[(2-hydroxyethyl)amino]benzyl alcohol (DIOL) from *m*-aminobenzyl alcohol with 2-chloroethanol. The mixture of *m*-aminobenzyl alcohol (6.84 g, 0.0324 mol) and 2-chloroethanol (4.61 g, 0.0573 mol) was stirred at 80 °C for 4 days under nitrogen bubbling in 1-butanol (100 mL) in the presence of potassium iodide (0.31 g, 0.001 87 mol) as a catalyst and potassium carbonate (5.59 g, 0.0404 mol) as an acid acceptor. In this reaction, the disubstituted byproduct of 3-[*N*,*N*-bis(2-hydroxyethyl)amino]-benzyl alcohol (TRIOL) was considerably produced. The reactant was analyzed by proton nuclear magnetic resonance (^{1}H-NMR) and reversed phase liquid chromatography (RPLC). ^{1}H-NMR and RPLC results exhibited that a considerable amount of TRIOL was produced in addition to the main product of DIOL. Thus, column chromatography was employed to isolate DIOL from the reactant mixture. After the chromatographic separation was carried out, the isolated DIOL compound was confirmed by the ^{1}H-NMR in acetone at 20 °C, as shown in Figure 2.

3-[(2-Hydroxyethyl)amino]-5-(hydroxymethyl)-4′-nitroazobenzene (T-AZODIOL). The diazonium coupling reaction[13] was employed to prepare T-AZODIOL and its reaction scheme is shown in Scheme 2. A solution of sodium nitrite (1.1 g, 0.016 mol) in 2.2 mL of water was added dropwise with stirring to a cooled solution of nitroaniline (2.07 g, 0.014 mol) in 35% hydrochloric acid (4.08 mL) and 12.4 mL of water at a temperature below 5 °C for 15 min. The obtained diazonium salt was coupled with isolated DIOL (2.5 g, 0.015 mol) in 1.54 mL of acetic acid solution at a temperature below 5 °C for 15 min. Then sodium acetate (1.05 g, 0.013 mol) was added, the solution was left in an ice bath for 1 h, additional sodium acetate (1.05 g, 0.013 mol) was added, and the reaction mixture was left for 0.5 h. After the temperature was raised to room temperature, a 20% sodium hydroxide solution (1.5 mL) was added and the whole mixture was left stirring at room temperature for 0.5 h. The resultant T-AZODIOL monomer was washed with water and filtered. Figure 2b shows the ^{1}H-NMR spectrum of T-AZODIOL measured in acetone at 20 °C. Elemental analysis gives the following composition ratio: C, 56.95; H, 5.10; O, 20.23; N, 17.72 this can be compared with the calculated one: C, 56.81; H, 4.84; O, 20.35; N, 17.08.

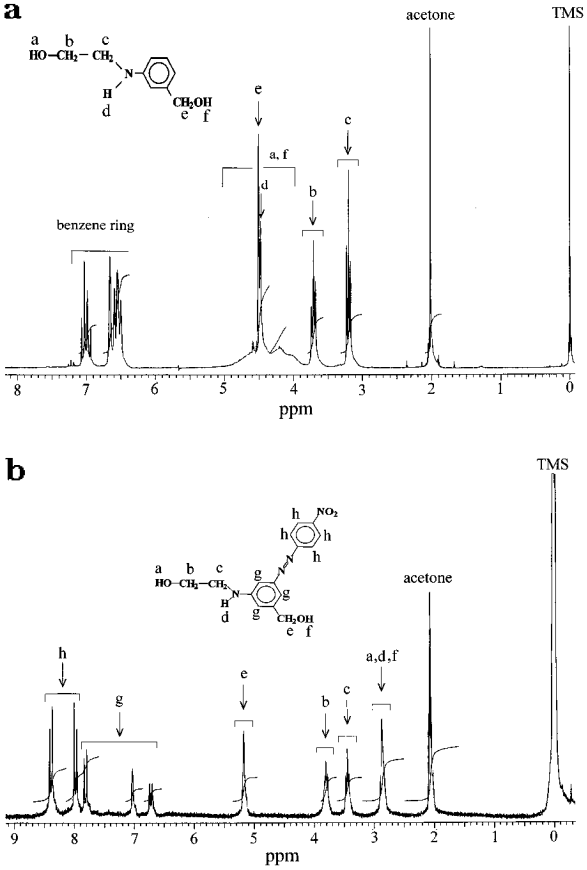

Figure 2. ^{1}H-NMR spectrum of DIOL (a) and ^{1}H-NMR spectrum of T-AZODIOL monomer (b).

Column Chromatography. The chromatographic separation was carried out on a column of silica gel (silica Gel 60 with particle size 0.063−0.23 mm, Merck) using acetonitrile as a developing solvent at room temperature. The elution rate was 5 mL/min.

Polymer Synthesis and Film Processing. T-AZODIOL and TDI with equivalent molar ratios were reacted in dimethylacetamide solution at 85 °C for 20 min in a nitrogen atmosphere to prepare T-polymer. L-polymer was prepared from AZODIOL with TDI using the same procedure described above. The spin-casting technique was employed to process thin films for SHG measurements.

Corona Poling. Spun-cast films were corona-poled at an elevated temperature to orient the NLO chromophore in the poling direction. The distance between the sample and 0.1 ∅ tungsten wire for corona poling was kept at 1.4 cm. Figure 3 illustrates the schematic pictures of aligned NLO chromophores induced by poling in T- and L-polymers. Schematic pictures give the idea that less deformation of the main chain in T-polymer than in L-polymer is expected.

SHG Measurements. The Maker fringe method[14,15] is employed to measure the SHG intensity of the poled spun-

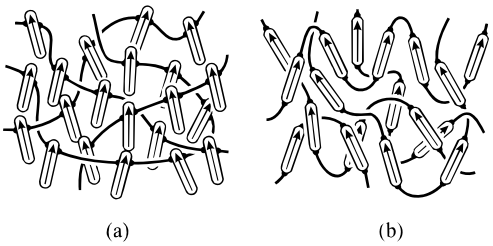

Figure 3. Schematic pictures of aligned NLO chromophores in T-polymer (a) and L-polymer (b).

cast films. The laser source is a Continuum model Surelite-10 Q-switched Nd:YAG pulse laser with a 1064 nm *p*-polarized fundamental beam (320 mJ maximum energy, 7 ns pulse width, and 10 Hz repeating rate). The generated second harmonic (SH) wave is detected by a Hamamatsu model R928 photomultiplier. The SH signal averaged on a Stanford Research Systems (SRS) model SR-250 gated integrator and boxcar averager module is transferred to a microcomputer through a SRS model SR-245 computer interface module. The details of the experimental procedure are described in refs 16 and 17.

Characterization. Reduced specific viscosity was measured in *N*,*N*-dimethylacetamide solution. The concentration of the polymer solution is 1.0 g/dL. Ultraviolet−visible spectra of the films were measured on a Shimadzu model UV-2101PC spectrophotometer. The m-line method using a prism coupling apparatus was employed to measure the refractive indices of the materials. Laser sources are a polarized He−Ne laser (632.8 nm) and a laser diode (830 nm). The prism of TaFD21 (HOYA Glass) with high a refractive index (1.925 88 at 632.8 nm) and a spin-coated or -cast film was coupled with a matching fluid of diiodomethane. Guided-wave spectra (m-lines) were obtained to determine the refractive indices. The nuclear magnetic resonance (NMR) spectrum was measured with TMS as an internal standard at 20 °C using a Varian model Gemini-200. Thermomechanical analysis (TMA) was performed in a penetration mode under a pressure of 10 kg/cm^2 and a heating rate of 10 °C/min in a nitrogen atmosphere, using a Seiko Instruments model TMA 100 thermomechanical analyzer controlled by a SSC-5200 disk station. Thermogravimetry (TG) was performed with a Shimadzu model DT-30 thermogravimetric analyzer at a heating rate of 10 °C/min in a nitrogen atmosphere. The density of the polymer film was measured in potassium iodide solution at 30 °C using a sink and float test.

Results and Discussion

Polymer Synthesis. Two types of urethane polymers, T-polymer and L-polymer, were prepared from T-AZODIOL and AZODIOL with TDI, respectively. Both polymers were prepared in dimethylacetamide at temperature of 85 °C for 20 min in nitrogen atmosphere. The resultant polymers have the reduced specific viscosities of 0.14 dL/g for T-polymer and 0.30 dL/g for L-polymer. The colored transparent thin films can be processed by spin-casting. The heat distortion temperature (T_h) determined by TMA measurement is used as a measure of the glass transition temperature (T_g) value for both polymers. T- and L-polymers had T_h values of 32−35 and 30 °C, respectively.

Absorption Spectra and Optimum Poling Condition for SHG. Figure 4 shows the absorption spectra of polymers before and after poling. Poling causes a decrease of absorption intensity and a shorter wavelength shift of the absorption maximum. Thermal annealing at the same temperature and time does not cause the intensity change and spectral shift. Thus, the intensity change is ascribed to the orientation of the azobenzene dye in the direction of the film thickness induced by poling. The spectral blue shift has been reported for other cross-linked main chain polymers,[8] which is in contrast to the red shift observed in most side-chain polymers.[18]

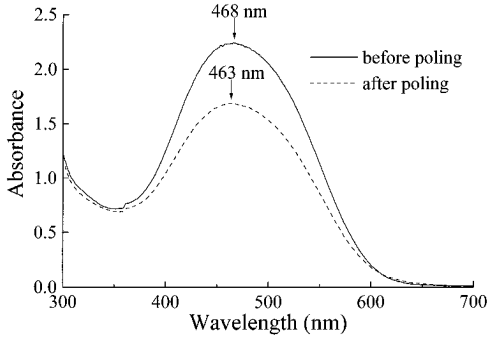

Figure 4. Absorption spectra of T-polymers before and after poling.

Table 1. RI Values at Wavelength of 632.8 and 830 nm Measured and Those at 532 and 1064 nm Predicted by Eq 1

	wavelength (nm)			
polymer	632.8	830	532	1064
T-polymer	1.6957	1.6686	1.779	1.661
L-polymer	1.6828	1.6499	1.745	1.638

It is important to optimize the poling conditions (poling voltage, temperature, and time) to obtain better SHG activities. For T-polymer, the SHG coefficient increased with increasing applied voltage and leveled out at the voltages above 8.0 kV. An increase of poling temperature causes an increase of the SHG coefficient with a large increase of the coefficient around 95 °C. The SHG coefficient poling time increased with and leveled out above 1 h. A poling voltage of 8.0 kV, a temperature of 95 °C, and a time of 60 min were the conditions employed for poling T-polymer. The details of the poling conditions of T-polymer have been reported in another paper.[19] For L-polymer, poling at the temperature above 70 °C caused the film surface to become opaque. The SHG coefficient increased with increasing applied voltage up to 7.0 kV, with its decrease above 8.0 kV. Then the poling of L-polymer was carried out at a poling voltage of 7.0 kV, a temperature of 62 °C, and s time of 60 min.

Refractive Indices and Determination of SHG Coefficients. The refractive indices (RI) for the transverse electric field (TE) mode are measured using the m-line method at wavelengths of 632.8 and 830 nm. RI values at wavelengths of 632.8 and 830 nm are listed for the unpoled polymer films in Table 1. The wavelength dispersion of RI, $n_f(\lambda)$, can be fitted to a one-oscillator Sellmeier-dispersion formula,

$$n_f^2(\lambda) - 1 = \frac{q}{1/\lambda_0^2 - 1/\lambda^2} + A \qquad (1)$$

where λ_0 is the absorption wavelength of the dominant oscillator, q is a measure for the oscillator strength, and A is a constant containing the sum of all the other oscillators. Figure 5 shows the plot of RI at wavelengths of 632.8 and 830 nm and the predicted curve of the wavelength dispersion of RI using eq 1 with $\lambda_0 = 470$

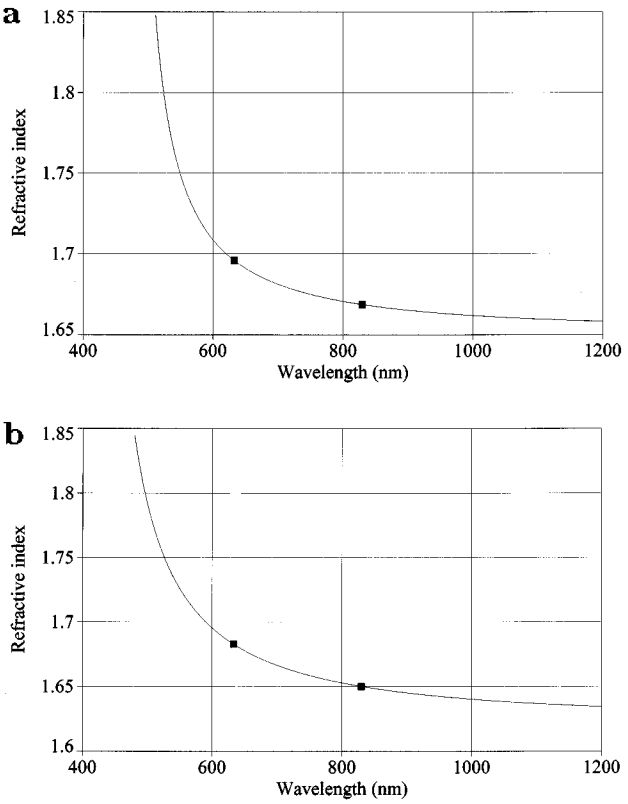

Figure 5. Plots of RI at the wavelength of 632.8 and 830 nm and the predicted plot curve of the wavelength dispersion of RI using eq 1 for T-polymer in (a) and for L-polymer in (b).

nm for T-polymer and $\lambda_0 = 414$ nm for L-polymer. RI values at 532 and 1064 nm obtained from the predicted plots are listed in Table 1 for both T-polymer and L-polymer, which are used for the calculation of the SHG coefficient.

The SHG coefficients of the polymers are made relative to a Y-cut quartz plate ($d_{11} = 1.2 \times 10^{-9}$ esu (0.5 pm/V)). The typical Maker fringe pattern could be observed for both the case of both *p*-polarized and *s*-polarized fundamental beams. When T-polymer film is poled at the optimum conditions of a poling voltage of 8.0 kV, a temperature of 95 °C, and a time of 60 min, a d_{33} value of 1.6×10^{-7} esu (67 pm/V) is obtained. This value is larger than the SHG coefficient of lithium niobate ($LiNbO_3$).

In the theoretical expression of SHG coefficient d_{33} can be written as

$$d_{33} = \frac{N_d f_\omega^2 f_{2\omega} \beta \mu_g E_p}{10kT} \tag{2}$$

where N_d is the number density of noncentrosymmetric NLO molecules, β is the hyperpolarizability of the NLO guest, f_ω and $f_{2\omega}$ are Lorentz−Lorenz local field factors of the form $(\epsilon + 2)/3$, μ_g is the dipole moment of the NLO chromophore at the ground state, E_p is the poling electric field, k is Boltzmann's constant, and T is the poling temperature. The value of ϵ has been taken as the square of the refractive index of the sample at either the fundamental or second harmonic frequency. The number density N_d is calculated using the film density. To evaluate d_{33} values from eq 2, β, μ_g, and E_p values must be estimated from the absorption spectra data.

E_p was determined from the intensity change in absorbance caused by the orientation of the NLO chromophore, using the electrochromic theory.[20,21] The orientation-induced intensity change in absorbance can be related to the electric field, using the electrochromic theory,

$$\frac{A(p)}{A(0)} = 1 - G(u) \tag{3}$$

where $A(p)$ and $A(0)$ are the absorbance with and without electric field, respectively, and

$$G(u) = 1 - \frac{3\coth(u)}{u} + \frac{3}{u^2} \tag{4}$$

and

$$u = \frac{\mu_g E_p}{kT} \tag{5}$$

β can be calculated using the two-level model,[22,23]

$$\beta = \frac{9e^2}{4m}\left(\frac{h}{2\pi}\right)^2 \frac{W}{[W^2 - (2h\nu)^2][W^2 - (h\nu)^2]} f\Delta\mu \tag{6}$$

where e is an elementary electric charge in esu, m is the rest mass of electron, h is Planck's constant, W is the energy at the absorption wavelength of the dominant oscillator, and $h\nu$ and $2h\nu$ are the energies of the fundamental and second harmonic light. f is the oscillator strength of the dominant oscillator and can be evaluated from the absorption spectrum of the dominant oscillator:[24,25]

$$f = \frac{2303mc^2}{\pi e^2 N n}\int \epsilon_{\tilde{\nu}}\, d\tilde{\nu} = 4.38 \times 10^{-9}\int \epsilon_{\tilde{\nu}}\, d\tilde{\nu} \tag{7}$$

where c is the speed of light, N is Avogadro's number, n is the refractive index which is commonly omitted from the above expression, $\epsilon_{\tilde{\nu}}$ is the molar extinction coefficient, and the integration is carried out over the absorption band of the dominant oscillator.

The β value is calculated using eq 6 with the dipole moment difference between the ground and excited states $\Delta\mu$ ($=\mu_e - \mu_g$) estimated from the well-known azobenzene dyes.[20] E_p is evaluated from the decrease of the absorption maximum using eq 3. Then, for T-polymer, d_{33} can be calculated as 1.0×10^{-7} esu by using $E_p = 2.7$ MV/cm from eq 3, $\mu_g = 8$ D,[20] and $\beta = 119 \times 10^{-30}$ esu from eq 6, which compares well with the experimentally obtained d_{33} which was 0.91×10^{-7} esu. The experimentally obtained d_{33} value is in good agreement with the theoretically calculated one.

Thermal Stability of SHG Activity. Figure 6 shows the long-term thermal stability of d_{33} for both T-polymer and L-polymer when the sample films were stored at room temperature for the times shown on the horizontal axis in the figure. The plot in the figure is of SHG coefficients d_{33} normalized by that measured at time zero. It is noted that T-polymer has a good long-term thermal stability of d_{33} (no significant relaxation at the ambient conditions in 60 days) except for the small activity loss within a few days after poling, whereas the SHG coefficient d_{33} of L-polymer has largely decreased day by day and reached a half the value at time zero after 2 weeks storage. Thus the difference of SHG activity profile against storage time

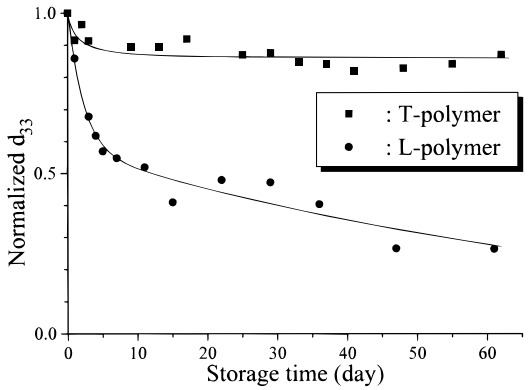

Figure 6. Long-term thermal stability of d_{33} values when T- and L-polymers are stored at room temperature.

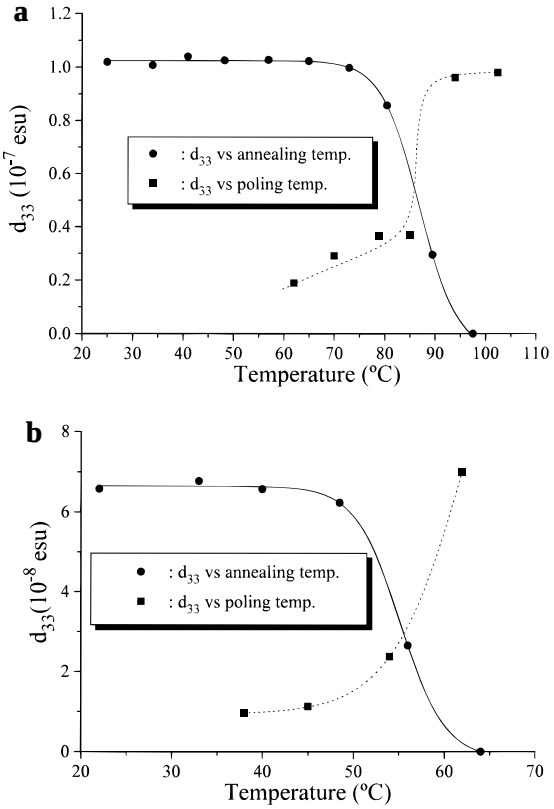

Figure 7. Temperature profile of d_{33} for T-polymer (a) and for L-polymer (b). The SHG measurement was carried out at the fixed temperature shown on the horizontal axis in the figure. The dotted curve is the d_{33} profile on poling, and the temperature on the horizontal axis in this curve is the poling temperature.

between T- and L-polymers is due to the difference of the mobility of the dipole moment between the two polymers.

Figure 7 shows the SHG activity profile vs annealing temperature for T-polymer (a) and L-polymer (b), respectively. Successive SHG measurements at higher fixed temperatures shown on the horizontal axis in the figure were carried out after both polymers were corona-poled. T-polymer does not show significant loss of SHG activity at temperatures up to 65 °C, and the large activity loss occurs at a temperature above 80 °C, whereas, for L-polymer, the initial SHG loss starts at a temperature around 40 °C. A significant large activity loss occurs around 50−55 °C. These temperature profiles of SHG activity also support the fact that T-polymer has a better thermal stability than L-polymer. It is noted that these SHG activity profiles vs annealing temperature can be compared to the SHG activity profiles when the poling temperature is raised, which are shown in dotted lines in Figures 7 (a,b). Values of d_{33} on poling drastically increase when the poling temperature increases from 85 to 95 °C for T-polymer and from 50 to 60 °C for L-polymer. Either poling temperature range in which the large increase of SHG activity occurs corresponds well to the fact that the SHG activity is significantly lost on annealing for each polymer. These coincidences imply that both processes of alignment (orientation) and randomization (reorientation) of the NLO chromophore should be subjected to the same thermal activation. In other words, the thermal mobility for aligning NLO dipole moments on poling is the same as that for randomizing them on annealing. According to this, the glass transition temperatures for the SHG activities are in the temperature range between 80 and 85 °C for T-polymer and between 50 and 55 °C for L-polymer. These transition temperatures are higher than those measured by TMA described above. This discrepancy may be related to the difference of mode in molecular motion which can be detected by each measurement. The details should be clarified by the further study using the dielectric relaxation and the thermal stimulated discharge current measurements.

Table 2. Density and Free Volume (V_f) Calculated by Eq 8 for T- and L-Polymers

	density (g/cm^3)	V_t (cm^3/g)	V_0 (cm^3/g)	V_f (cm^3/g)
T-polymer	1.246	0.803	0.632	0.171
L-polymer	1.147	0.872	0.662	0.210

The question arising is what is the origin of stabilizing NLO dipole moments in T-polymer? One possibility is the free volume of the matrix which provides the free space where the aligned dipole moment can be thermally reoriented. The density of T-polymer is larger than that of L-polymer, as shown in Table 2. The larger density of T-polymer leads to the smaller free volume of T-polymer. The free volume V_f can be estimated from the experimentally obtained specific volume V_t (the reciprocal value of measured density) and the zero point molar volume V_0,

$$V_f = V_t - V_0 \tag{8}$$

where V_0 can be calculated from the van der Waals volume V_w of the polymer, $V_0 = 1.3V_w$.[26] V_w of polymers was determined by the summation of the van der Waals volumes of group contributions.[27] Table 2 shows the free volumes of T- and L-polymers calculated. As expected, V_f of T-polymer is smaller than that of L-polymer. Thus, the smaller free volume of T-polymer significantly contributes to the restriction of molecular motion in the glassy state of the matrix. That is, the orientation of the NLO chromophore in T-polymer is sustained by the smaller free volume of matrix in T-polymer.

The detailed studies of the thermal relaxation of SHG activities for both T- and L- polymers and their relation to the orientation of NLO dipole moments are in progress and will be published in the future.

Conclusion

A novel class of NLO polymer, T-polymer, for SHG is presented. This novel class of NLO polymer has large a dipole moment which is aligned transverse to the main chain backbone. This polymer is amorphous with a high

density of NLO chromophore moieties and an optically transparent thin film can be processed by spin-casting. Poled T-polymer shows a large second-order nonlinearity of $d_{33} = 1.6 \times 10^{-7}$ esu (67 pm/V). A good thermal stability of nonlinearity was observed at ambient conditions. The better thermal stability of T-polymer is related to the smaller free volume in T-polymer.

Acknowledgment. We are sincerely grateful to Prof. Murakami, Department of Polymer Science & Engineering, Kyoto Institute of Technology, for the facility and measurement of RPLC and fruitful advice for RPLC analysis and to Mr. Shuji Yoshizaki, graduate student in our laboratory, for preparation of the AZO-DIOL monomer.

References and Notes

(1) Meredith, G. R.; Van Dusen, J. G.; Williams, D. J. *Macromolecules* **1982**, *15*, 1385.
(2) Hampsch, H. L.; Yang, J.; Wong, G. K.; Torkelson, J. M. *Macromolecules* **1988**, *21*, 526.
(3) Singer, K. D.; Sohn, J. E.; Lalama, S. J. *Appl. Phys. Lett.* **1986**, *49*, 248.
(4) Eich, M.; Sen, A.; Looser, H.; Bjorklund, G. C.; Swalen, J. D.; Twieg, R.; Yoon, D. Y. *J. Appl. Phys.* **1989**, *66*, 2559.
(5) Wang, C. H.; Guan, H. W. *J. Polym. Sci., Part B: Polym. Phys.* **1993**, *31*, 1983.
(6) Eich, M.; Reck, B.; Yoon, D. Y.; Willson, G. C.; Bjorklund, G. C. *J. Appl. Phys.* **1989**, *66*, 3241.
(7) Jungbauer, D.; Reck, B.; Twieg, R.; Yoon, D. Y.; Willson, C. G.; Swalen, J. D. *Appl. Phys. Lett.* **1990**, *56*, 2610.
(8) Ranon, P. M.; Shi, Y., Steier, W. H.; Xu, C.; Wu, B.; Dalton, L. R. *Appl. Phys. Lett.* **1993**, *62*, 2605.
(9) Boogers, J. A. F.; Klaase, P. Th. A.; de Vliger, J. J.; Tinnemans, A. A. *Macromolecules* **1994**, *27*, 205.
(10) White, K. M.; Francis, C. V.; Isackson, A. J. *Macromolecules* **1994**, *27*, 3619.
(11) Tsutsumi, N.; Yoshizaki, S.; Sakai, W.; Kiyotsukuri, T. *Macromolecules* **1995**, *28*, 6437.
(12) Wender, C.; Neuenschwander, P.; Suter, U. W.; Prêtre, P.; Kaatz, P.; Günter, P. *Macromolecules* **1994**, *27*, 2181.
(13) S'heeren, G.; Persoons, A.; Bolink, H.; Heylen, M.; Van Beylen, M.; Samyn, C. *Eur. Polym. J.* **1993**, *29*, 981.
(14) Maker, P. D.; Terhune, R. W.; Nisenoff, M.; Savage, C. M. *Phys. Rev. Lett.* **1962**, *8*, 21.
(15) Jerphagnon, J.; Kurtz, S. K. *J. Appl. Phys.* **1970**, *40*, 1667.
(16) Tsutsumi, N.; Ono, T.; Kiyotsukuri, T. *Macromolecules* **1993**, *26*, 5447.
(17) Tsutsumi, N.; Fujii, I.; Ueda, Y.; Kiyotsukuri, T. *Macromolecules* **1995**, 28, 950.
(18) Page, R. H.; Jurich, M. C.; Reck, B.; Sen, A,; Twieg, R. J.; Swalen, J. D.; Bjorklund, G. C.; Willson, C. G. *J. Opt. Soc. Am. B* **1990**, *7*, 1239.
(19) Tsutsumi, N.; Matsumoto, O.; Sakai, W.; Kiyotsukuri, T. *Appl. Phys. Lett.* **1995**, *67*, 2272.
(20) Liptay, W. In *Exited States;* Lim, E. C., Ed.; Academic Press: New York and London, 1974; Vol. 1, pp 129−229.
(21) Havinga, E. E.; van Pelt, P. *Ber. Bunsen-Ges. Phys. Chem.* **1979**, *83*, 816.
(22) Oudar, J. L.; Chemla, D. S. *J. Chem. Phys.* **1977**, *66*, 2664.
(23) Levine, B. F.; Bethea, C. G. *J. Chem. Phys.* **1978**, *69*, 5240.
(24) Turro, N. J. In *Modern Molecular Photochemistry*; Benjamin/Cummings Publishers: Menlo Park, CA, 1978; pp 86−87.
(25) Birks, J. B. In *Photophysics of Aromatic Molecules*; John Wiley & Sons: London and New York, 1970; pp .51−52.
(26) Bondi, A. In *Physical Properties of Molecular Crystals, Liquids and Glasses;* John Wiley & Sons: New York, 1968; Chapters 3 and 4.
(27) van Krevelen, D. W. In *Properties of Polymers;* Elsevier: Amsterdam, 1990; Chapter 4.

MA951077O